Available online at www.sciencedirect.com
ScienceDirect
Polymer 48 (2007) 2022–2029
polymer
www.elsevier.com/locate/polymer

Broadband dielectric spectroscopic characterization of the hydrolytic degradation of carboxylic acid-terminated poly(D,L-lactide) materials

Mohammad K. Hassan[1], Jeffrey S. Wiggins, Robson F. Storey, Kenneth A. Mauritz*

The University of Southern Mississippi, School of Polymers and High Performance Materials, 118 College Drive, Hattiesburg, MS 39406-0076, United States

Received 20 December 2006; accepted 20 January 2007
Available online 30 January 2007

Abstract

Broadband dielectric spectroscopy was used to examine carboxylic acid-terminated poly(D,L-lactide) samples that were hydrolytically degraded in 7.4 pH phosphate buffer solutions at 37 °C. The dielectric spectral signatures of degraded samples were considerably more distinct than those of undegraded samples and a T_g-related relaxation associated with long range chain segmental mobility was seen. For both degraded and undegraded samples, a relaxation peak just beneath a DSC-based T_g was observed, which shifts to higher frequency with increasing temperature. Thus, this feature is assigned as the glass transition as viewed from the dielectric relaxation perspective. Linear segments on log–log plots of loss permittivity vs. frequency, in the low frequency regime, are attributed to d.c. conductivity. An upward shift in relaxation peak maximum, f_{max}, observed especially after 145 d of immersion in buffer, implies a decrease in the time scale of long range segmental motions with increased degradation time.

Permittivity data for degraded and undegraded materials were fitted to the Havriliak–Negami equation with subtraction of the d.c. conductivity contribution to uncover pure relaxation peaks. Parameters extracted from these fits were used to construct Vogel–Fulcher–Tammann–Hesse (VFTH) curves and distribution of relaxation time, $G(\tau)$, curves for all samples. It was seen that the relaxation times for the α-transition in both degraded and undegraded samples showed VFTH temperature behavior. $G(\tau)$ curves showed a general broadening and shift to lower τ with degradation, which can be explained in terms of a broadening of molecular weight within degraded samples and faster chain motions.

Keywords: Broadband dielectric spectroscopy; Poly(D,L-lactide); Hydrolytic degradation

1. Introduction

Biodegradable polyesters and co-polyesters have been the focus of extensive research for several decades as a result of their ease of manufacturing and desirable characteristics. Degradation mechanisms vary among biodegradable polyesters depending on chemical composition and are typically categorized as hydrolytic and/or microbial. Factors that influence degradation rate include material hydrophilicity, morphology, end group type, crosslink density, and surface chemistry. Additives such as monomers, acidic or basic compounds, superoxide ions, drugs or other active ingredients, and catalysts have all been shown to influence degradation kinetics [1]. In general, many studies have shown that the presence of free carboxylic acid moieties, whether on the end group of the polymer or blended into the sample as an additive or active ingredient, will accelerate the hydrolytic degradation rates of polyesters [1–5].

Modern broadband dielectric spectroscopy has proved to be a useful tool to study the molecular dynamics of polymers due to the fact that response over a broad frequency range from the milli- to giga-Hertz region can be tested. Therefore, motional processes which take place for polymeric systems on extremely different time scales can be investigated over a broad

* Corresponding author. Tel.: +1 601 266 5595; fax: +1 601 266 5504.
E-mail address: kenneth.mauritz@usm.edu (K.A. Mauritz).
[1] Permanent address: Bani Suef University, Faculty of Science, Chemistry Department, Bani Suef, Egypt.

0032-3861/$ - see front matter © 2007 Elsevier Ltd. All rights reserved.
doi:10.1016/j.polymer.2007.01.054

frequency and temperature ranges. Moreover, the motional process can depend on the morphology of the system under investigation. Therefore, information on the structural state of the material can be indirectly extracted by taking the molecular mobility as a probe of the structure [6].

Molecular motions in amorphous entangled polymer chains can have considerable restrictions and exist on very different time and length scales; therefore, different vector components that contribute to the net dipole moment can undergo reorientation in different motional processes. Thus, the dielectric spectrum of an amorphous polymer generally shows multiple relaxations, depending on temperature, where each process is indicated by a peak in loss permittivity (ε'') in the frequency and temperature domains and an associated step decrease in storage permittivity (ε') vs. frequency (f) at a fixed temperature. Most amorphous polymers exhibit a secondary β-relaxation in the glassy state and a primary α-relaxation (dynamic glass transition) at lower frequencies (or higher temperature) than the β-relaxation. Useful information on the structural and dynamic states of a polymeric material can be extracted by monitoring macromolecular mobility in this way. The structural aspect of interest in these studies is the molecular weight distribution as affected by degradation.

Henry et al. analyzed the β-relaxation, observed between −150 and −30 °C depending on the measurement frequency, for industrial and purified poly(lactic acid) samples [7]. They assigned this process to be a secondary relaxation in the glassy state and investigated its change with degradation resulting from sample exposure to a controlled atmosphere with relative humidity of 78% at 25 °C. This β-relaxation was assigned to local motional processes associated with the terminal polar carboxylic acid groups. This study did not reveal any analysis of the higher temperature glass transition-related α-relaxation which will be mainly the subject of the study reported here, in which the conditions for hydrolytic degradation are more severe.

This work reports the use of modern broadband dielectric spectroscopy as a novel approach in the study of the degradation of carboxylic acid-terminated poly(D,L-lactide) materials from the perspective of modified macromolecular motions. As this technique is largely unfamiliar to the community engaged in the pursuit of biodegradable materials, fundamental explanations are provided where needed in this presentation.

This report contains the dielectric spectroscopic analysis of three samples, two degraded for considerably different times as well as that of an undegraded control sample. It was decided to initially present the results for this limited number of samples to primarily demonstrate the ability of this method to diagnose changes in polymer chain dynamics in some detail. The number of samples was also limited owing to the large number of parameters that issue from the spectroscopic analysis in addition to the fact that there are a large number of experimental variable possibilities.

The analysis outlined here can be considered as useful in a broader context of materials that are chemically degraded in similar ways, an example being proton exchange membranes that are exposed to generated peroxide in fuel cells.

2. Experimental

2.1. Materials and degradation study

The biodegradable polyester material used in this study, described in a previous report [5], is carboxylic acid-terminated poly(D,L-lactide) having a number average molecular weight of 20,000 g/mol. These materials were degraded by exposure to phosphate-buffered aqueous solutions (7.4 pH, 0.05 M) at 37 °C for different time intervals up to 180 d and were tested for relative moisture uptake and weight loss behaviors. Sample discs of diameter 2.54 cm and thickness of ~1 mm were prepared for degradation studies by melt pressing them at 100 °C for 15 min.

2.2. Sample preparation and dielectric spectroscopic measurements

Dielectric relaxation spectra were collected using a Novocontrol GmbH Concept 40 broadband dielectric spectrometer over the frequency range 0.01 Hz−3 MHz and over the temperature range of 0−100 °C. The temperature stability of the instrument was controlled to be within ±0.2 °C.

Degraded sample discs were carefully dried by melting at 100 °C for 20 min under vacuum to remove residual moisture that might cause further degradation. The discs were then melt pressed between two gold coated copper electrodes at 100 °C using a hot press. This process was done in two steps using polyimide non-stick films between the sample and one of the electrodes to visually examine the sample while it was attached to the other electrode. This procedure allowed for inspection of possible air bubbles in the sample before conducting the dielectric spectroscopy experiment. The upper electrode was 2 cm in diameter and the lower electrode was 3 cm in diameter.

3. Results and discussion

3.1. Dielectric spectra of unhydrolyzed polymers

The glass transition peak and shift of the associated relaxation time to shorter values with increasing temperature are seen in ε'' vs. f plots for the same sample at different temperatures, in Fig. 1. There is a relaxation peak in the vicinity of, and just beneath the temperature of a previously determined, DSC-based glass transition ($T_g = 48$ °C at transition midpoint) [5], which becomes more distinct and shifts to higher f with increasing temperature. A relaxation time, τ_{max}, can be extracted as usual from the frequency corresponding to the peak maximum, f_{max}, as $\tau_{max} = (2\pi f_{max})^{-1}$. Havriliak and Negami pointed out that the value of f for which ε'' is maximum is not exactly the relaxation time for cases for which the Cole−Cole plots (ε'' vs. ε') [8] are not strict semicircles but rather are arcs skewed toward the left, that is, in the progression of increasing f [9−11]. When such curve asymmetry exists, the actual relaxation time is longer than that derived from the condition $\partial\varepsilon''/\partial\omega = 0$, where $\omega = 2\pi f$.

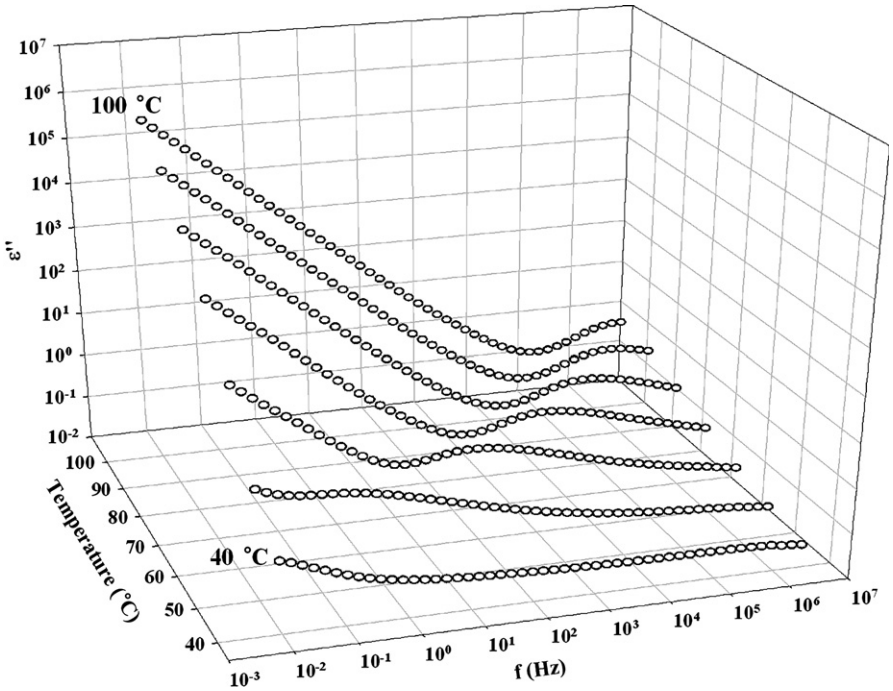

Fig. 1. Dielectric loss spectra of undegraded 20 kg/mol COOH chain-terminated poly(D,L-lactide) samples. The curves are spaced at 10 °C increments from 40 to 100 °C.

In the low-f region and for $T > T_g$ the $\log_{10}\varepsilon''$ vs. $\log_{10} f$ plots are linear with calculated slopes being slightly less than 1.0. This reflects d.c. conductivity which is characterized by the relationship $\varepsilon''_{dc} = G_{dc}/(\omega C_0)$, where G_{dc} is the d.c. conductance and C_0 is the vacuum capacitance for the unfilled cell in which the electrode plate spacing is equal to the sample thickness [12]. For 'ideal' conduction the d.c. curve segment is characterized by the relationship $\varepsilon'' \propto \omega^{-1}$ but often the general power law $\varepsilon'' \propto \omega^{-N}$, where N is the slope of the line, is obeyed. An additional spectral feature, caused by sample–electrode interfacial polarization can be present as characterized by N being considerably less than 1.00 and ε' being inordinately large with decreasing f at the lowest frequencies. This effect was discussed in reports of dielectric relaxation studies of hydrated perfluorosulfonate ionomer membranes [13–18].

3.2. Dielectric spectra of hydrolyzed polymers

Fig. 2 consists of $\log_{10}\varepsilon''$ vs. $\log_{10} f$ plots for a dried 20 kg/mol acid-terminated sample that was immersed in buffer solution for 75 d at 37 °C. After the hydrolysis reaction was terminated, the samples were melted under vacuum at 100 °C to remove residual water before the dielectric spectroscopic analysis. In addition to minimizing the obscuring effect of d.c. conductivity due to residual water, this procedure was also critical for removing surface voids, caused by degradation/erosion, which would have compromised the intimacy of contact between sample and electrode. Although the original degraded morphology is destroyed, the dielectric relaxation associated with the glass transition is mainly dependent on molecular weight, which is reduced by hydrolytic scission along the chain.

The overall trend of higher f_{max} with increasing temperature is similar to that for the untreated sample. As in Fig. 1, there is an upward vertical curve displacement with increasing temperature although ε'' attains considerably higher values than those for the untreated sample in the low frequency regime. This, as well as an enhanced polarizability that is evidenced by an upward vertical displacement of the ε' vs. f curves (data not shown), could be due to the hydrolytic cleavage of main chain ester linkages which increases the number density of polar carboxylic acid end groups.

3.3. Effect of degradation time on dielectric relaxation spectra

Fig. 3 shows $\log_{10}\varepsilon''$ vs. $\log_{10} f$ curves at 60 °C for dried 20 kg/mol COOH chain-terminated samples that were immersed in buffer solution for 75 and 145 d at 37 °C as well as an untreated control sample. At 60 °C, which is considerably above T_g for the untreated sample, f_{max} associated with the time scale of long range segmental motions increases with increased degradation time. This behavior reflects an increase in chain segmental motion caused by molecular weight degradation. The shift in f_{max} is not great up to 75 d, which correlates with our previous observation that there is low percent weight loss for the same sample up to this degradation time [5], and this would imply that there was no significant downward shift in molecular weight within this period. Moreover, this peak is broader at 145 d which suggests a broader distribution of relaxation times with greater degradation.

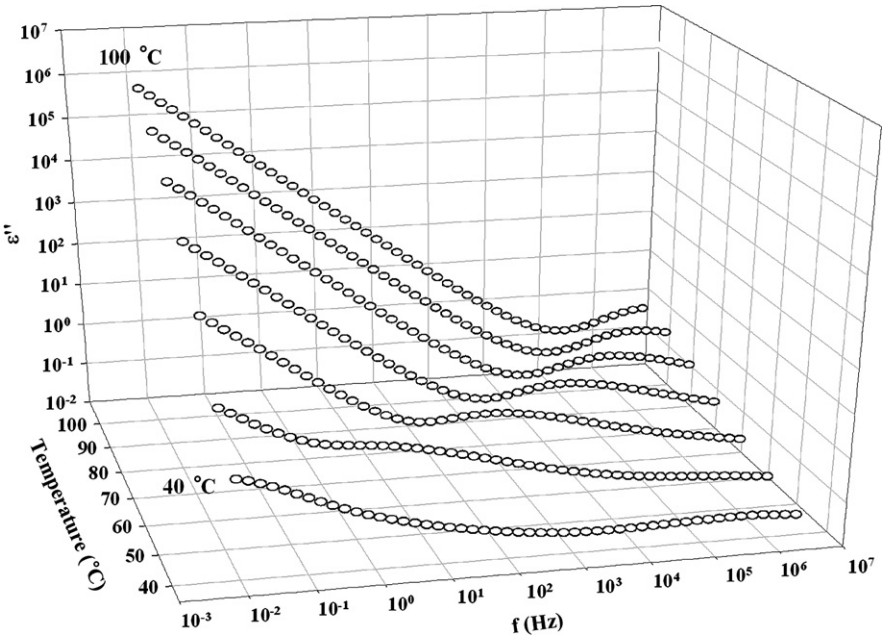

Fig. 2. $\log_{10}\varepsilon''$ vs. $\log_{10} f$, at various fixed temperatures, for a dry 20 kg/mol COOH chain-terminated sample that underwent degradation by hydrolysis for 75 d at 37 °C.

Also, degradation caused a vertical upward displacement of curves in the low-f region, especially after 145 d immersion time. This, again, reflects increased density of polar carboxylic acid end groups with increased degradation.

Jamshidi et al. [19] established that T_g vs. number average molecular weight (M_n) for poly(lactic acid) follows the Flory–Fox relationship [20,21]:

$$T_g = T_g^{\infty} - K/M_n \tag{1}$$

K is a constant for the particular polymer and T_g^{∞} is the hypothetical glass transition temperature at infinite molecular weight. These investigators found that T_g^{∞} for poly(D,L-lactide) and poly(L-lactide) is 57 and 58 °C, respectively. While this equation is largely empirical, it can be rationalized on the basis of excess free volume associated with the packing of chains around chain ends, although intra- and inter-chain polar and hydrogen bonding interactions would be expected to influence T_g as well. In any case, the established validity of this equation for these polymers allows for interpreting upward shifts in the T_g-related f_{max} with a decrease in average molecular weight due to polymer chain degradation.

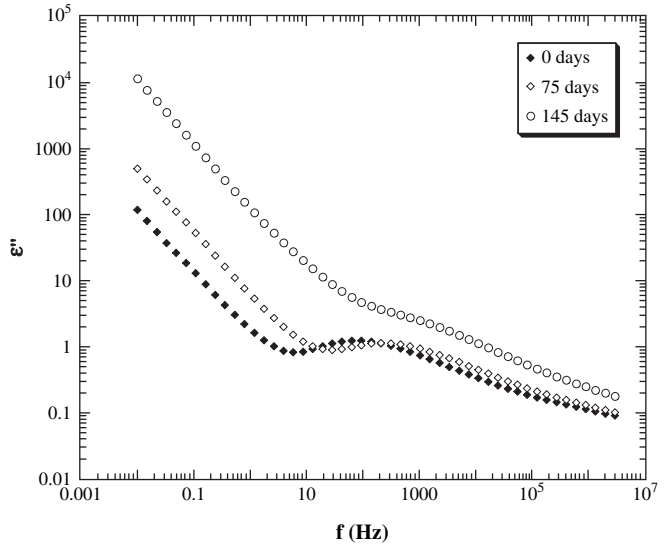

Fig. 3. $\log_{10}\varepsilon''$ vs. $\log_{10} f$ plots, at 60 °C, for dry 20 kg/mol COOH chain-terminated samples that underwent degradation for 75 and 145 d as well as for a corresponding untreated sample.

An alternate explanation of these results comes from the perspective of the Rouse–Zimm model that predicts that the relaxation time for simple polymers above T_g is directly proportional to the product of the molecular weight and viscosity, where the latter increases with increasing molecular weight [12, p. 147].

With either view, complications caused by water plasticization can be discounted because the samples were carefully dried.

Linear low frequency upturns to the left of the relaxation peaks observed in Fig. 3, attributed to d.c. conduction, are displaced upward with increasing degradation time. While the exact nature of the charge carrier in the conduction process is not clear, an increasing density of COOH groups resulting from ester linkage hydrolysis with increased chain scission must be implicated. d.c. conductivity, in essence, involves the sampling of charge hopping pathways that become progressively longer at increasingly lower frequencies. As the experimental time scale, or half period of oscillation $= (2f)^{-1}$, increases, charge carriers, possibly protons in this case, can execute more elementary hops throughout the free volume of the polymer before the applied field reverses. This phenomenon likely reflects an increase in the number of carboxylic end groups as hydrolytic degradation progresses.

3.4. Data analysis using the Havriliak–Negami (HN) and Vogel–Fulcher–Tammann–Hesse (VFTH) equations

In order to extract more information on degraded chemical structure and chain dynamics, the phenomenological Havriliak–Negami (HN) equation was fitted to the permittivity data shown in Figs. 1 and 2 [9–11]:

$$\varepsilon^*(\omega) = \varepsilon' - i\varepsilon'' = -i\left(\frac{\sigma_0}{\varepsilon_0\omega}\right)^N + \sum_{k=1}^{3}\left[\frac{\Delta\varepsilon_k}{(1+(i\omega\tau_{\mathrm{HN}})^{\alpha_k})^{\beta_k}} + \varepsilon_{\infty k}\right] \tag{2}$$

$\Delta\varepsilon_k = (\varepsilon_R - \varepsilon_\infty)_k$, the difference between the real permittivities (ε') at very low and very high frequencies, respectively, is the relaxation strength for the kth relaxation and ε_0 is the vacuum permittivity. Depending on the complexity of the spectra, one, two or three relaxation terms in the summation may be used in the curve fit. τ_{HN} is the Havriliak–Negami relaxation time, and α and β ($0 < \alpha < 1$, $\alpha\beta \leq 1$) are permittivity vs. ω curve shape constants where α quantifies the breadth of the distribution of relaxation times and β accounts for distribution asymmetry for the kth relaxation. σ_0 is the d.c. conductivity in units of S/cm. The exponent N ($0 < N \leq 1$) that was to referred earlier characterizes the conduction process in terms of charge hopping pathways and mobility constraints. σ_0, N, τ_{HN}, $\Delta\varepsilon$, α, and β are treated as free variables that are obtained by fitting the HN equation to the loss permittivity (ε'') spectra. Curve fitting was performed using the WinFit program (Novocontrol) and the parameters extracted from fitting the data for this system are listed in Table 1. τ_{HN} is related to $\tau_{\max}$ by the following equation [6, p. 64]:

$$\tau_{\max} = \tau_{\mathrm{HN}}\left[\frac{\sin\left(\frac{\pi\alpha\beta}{2(\beta+1)}\right)}{\sin\left(\frac{\pi\alpha}{2(\beta+1)}\right)}\right]^{\frac{1}{\alpha}} \tag{3}$$

Note that $\tau_{\mathrm{HN}} = \tau_{\max}$ when $\beta = 1$.

The first d.c. conductivity term in Eq. (2) is not a relaxation but a spectral-obscuring factor that is subtracted for the purpose of uncovering the actual relaxation signatures of macromolecular motions. This subtraction is especially necessary to resolve the relaxation times at temperatures approaching T_g at which d.c. conduction becomes stronger [22]. Even in the absence of intended ions, water, or in some rare cases, free electrons, there can be unknown impurity charges in a polymer and a low concentration of these is sufficient for this effect to be seen.

As seen in the d.c.-subtracted spectra in Fig. 4 for the fixed temperature of 60 °C, $f_{\max}$ shifts to higher values with increased time of degradation. Accordingly, $\tau_{\max} = 1/(2\pi f_{\max})$ decreases by decades, reflecting more rapid chain motions. There is a broadening of this peak with degradation, especially after 145 d. We suggest that this is caused by a broadening of the distribution of molecular weights in the sense that smaller degraded macromolecular fragments have greater motional freedom than undegraded chains. As mentioned, the Rouse–Zimm model predicts that the relaxation time for long range chain motions in the rubbery state is directly proportional to molecular weight and viscosity, where the latter increases with increasing molecular weight [12, p. 147]. Hence, if the average molecular weight shifts to lower values through degradation, $f_{\max}$ will necessarily shift to higher values.

Segmental relaxation is a non-Arrhenius process having a relaxation time, τ, that has a temperature dependence that follows the Vogel–Fulcher–Tammann–Hesse (VFTH) equation [23]:

$$\tau(T) = \tau_0 \exp\left(\frac{E_a}{k_B(T - T_V)}\right) \tag{4}$$

k_B is the Boltzmann constant and τ_0, E_a, and T_V are treated as parameters obtained by fitting Eq. (4) to experimental data. τ_0 is a hypothetical relaxation time at infinite temperature. E_a, while having units of energy, is a quantity of uncertain meaning that is not associated with an activated process in the usual sense and can, in fact, have values that are unrealistically high, for example, much greater than the binding energy for a C–C bond near the glass transition [24]. T_V, the Vogel temperature,

Table 1
Havriliak–Negami and VFTH fit parameters for dielectric spectra at 60 °C for samples degraded for 75 and 145 d, as well as for an undegraded control sample

Sample	Relaxation time[a] (s)	α	β	T_V (K)
Undegraded	2.42×10^{-3}	0.59	0.73	281
75 d degraded	4.39×10^{-4}	0.71	0.80	255
145 d degraded	3.72×10^{-4}	0.65	0.63	292

[a] As calculated by Eq. (3).

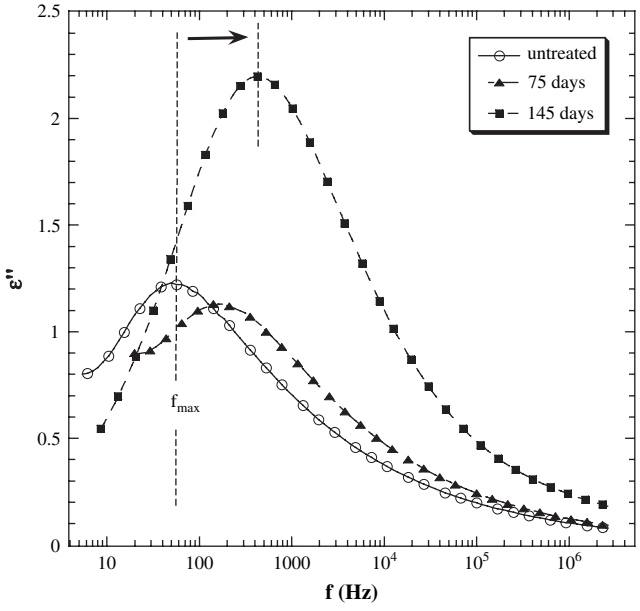

Fig. 4. ε'' vs. $\log_{10} f$, at 60 °C, for dry 20 kg/mol COOH-terminated samples that underwent degradation for 75 and 145 d as well as for a corresponding untreated sample with the conductivity contribution subtracted.

can be viewed as the temperature at which chain segments become immobile, or frozen-in, in a hypothetical situation in which a polymer is cooled at a very slow (quasi-static) rate from the rubbery state. Given this prescription, T_V is expected to be lower than T_g according to the following equation [6, p. 103]:

$$T_V = T_g - \frac{f_g}{\alpha_f} \tag{5}$$

f_g is the free volume fraction at T_g and α_f is the temperature coefficient of free volume expansion. For quasi-static cooling, in the absence of kinetic effects inherent in all rate-dependent experiments to determine T_g, f_g would be zero and $T_V = T_g$ in this hypothetical limit.

Fig. 5 shows the VFTH plots for the untreated and 75 and 145 d degraded samples. The plots are not linear, i.e., non-Arrhenius like, which indicates that this is not a process that can be described in terms of conventional activated rate theory. Also, there is a distinct separation between the curves for the undegraded and degraded samples. The VFTH equation can be well fitted to the data for both degraded and undegraded samples as in cases for the α-transition of other polymers [12]. Curve-fitted values of the VFTH parameters for this system are listed in Table 1. T_V decreased with immersion in buffer for 75 d and then increased for 145 d immersion. T_V would be expected to decrease with increased degradation time as the free volume increases, and it was discussed above how smaller, degraded chains insert more excess free volume into the system.

While it is not entirely clear as to why T_V increased after 145 d, an explanation is offered based on the idea that generated low molecular weight chains, i.e., oligomers, can solubilize and leach out of the sample during the degradation experiment. These soluble chains could act as packing defects, the absence of which would cause the longer chains to pack more efficiently, and there would be a resultant redistribution of free volume. On the other hand, a broadening of molecular weight distribution with increased degradation time would not be in harmony with this view. Another explanation is based on the fact that the number of carboxylic acid groups at the chain ends increases with increased degradation. Increased hydrogen bonding between chains in this way would restrict their mobility which would have the same effect as a decrease in free volume. Thus, the number of hydrogen-bonded chains increases and chain mobility becomes more restricted which would have the same effect as a decrease in free volume [25].

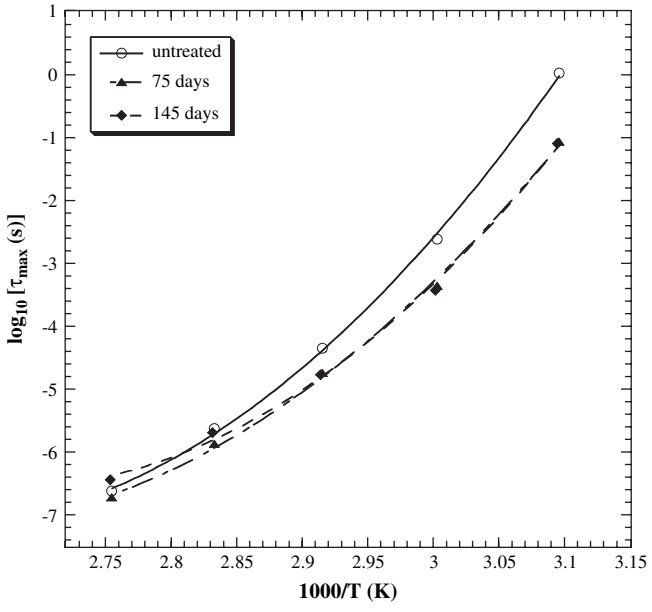

Fig. 5. VFTH plots at 60 °C for samples degraded for 75 and 145 d as well as an undegraded control sample.

3.5. Effect of degradation on the distribution of relaxation times

In the Havriliak–Negami treatment α and β determine the distribution of relaxation times, $G(\tau)$. α characterizes the breadth of the distribution while β characterizes the extent of skew from curve symmetry by its deviation from the value of 1 [10]. $G(\tau)$ is given by the following equation [10]:

$$G(\tau) = \frac{\left(\frac{\tau}{\tau_{0i}}\right)^{\beta_i\alpha_i} \sin(\beta_i\Theta_i)}{\pi\tau\left(\left(\frac{\tau}{\tau_{0i}}\right)^{2\alpha_i} + 2\left(\frac{\tau}{\tau_{0i}}\right)^{\alpha_i}\cos(\pi\alpha_i) + 1\right)^{\frac{\beta_i}{2}}} \tag{6}$$

In Eq. (6),

$$\Theta_i = \arctan\left(\frac{\sin(\pi\alpha_i)}{\left(\frac{\tau}{\tau_{0i}}\right)^{\alpha_i} + \cos(\pi\alpha_i)}\right)$$

The quantity Θ_i has units of an angle in radians such that $(0 \le \Theta_i \le \pi)$.

$G(\tau)$ plots for degraded vs. non-degraded samples are shown in Fig. 6. The obscuring d.c. contribution has been subtracted from the loss spectra so that only pure relaxation effects are present. There is distinct peak broadening but with less asymmetry with increasing degradation time. This, according to the rationale presented above, is interpreted in terms of molecular weight degradation and molecular weight distribution broadening with time. The shift in curve maximum to lower τ reflects faster chain motions as would be expected for shorter chains. It is also seen that α, β and $G(\tau)$ are temperature dependent (data not shown).

In polymer blends, relaxation peak broadening is usually attributed to two mechanisms: concentration fluctuation and intrinsic mobility differences between the blend components [25]. Within the context of this system, at some degradation stage, one can consider a 'blend' of chains of lengths that are so diverse as to create microstructural heterogeneity, in part because the solubility of chains depends on molecular weight and the effect is more pronounced for shorter chains. Thus, there will also be distribution in chain dynamics, i.e., relaxation times.

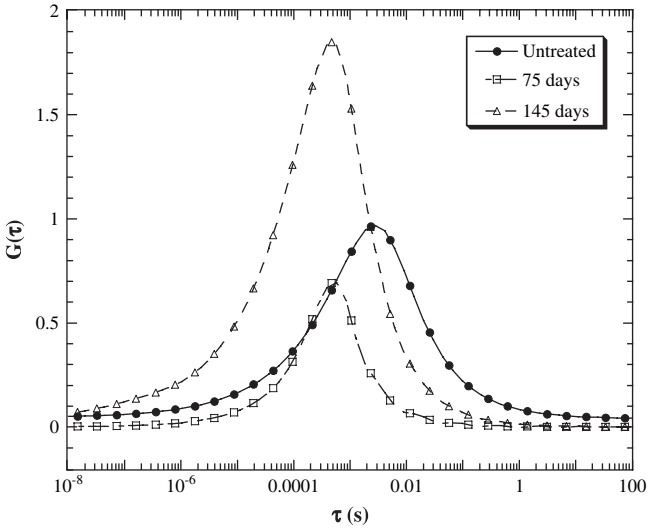

Fig. 6. Distribution of relaxation times at 60 °C for an untreated sample and samples degraded for 75 and 145 d.

In a concentration fluctuation model, Fisher and co-workers assumed that there are many dynamically heterogeneous domains in polymer blends. Different domains have different compositions which are assumed to follow a Gaussian distribution centered around the global composition [26,27]. Roland and Ngai modeled the dynamics of polyisoprene/poly(vinylethylene) blends by assuming that concentration fluctuations lead to normally distributed coupling parameters for each blend component and the observed relaxation time distribution is a summation of all of these components [28]. It should be noted that intermolecular hydrogen bonding is capable of damping concentration fluctuations [25], which could be true for the present system as the number of carboxylic acid groups increases with degradation due to ester linkage hydrolysis. The geometric distribution of hydrogen bonding throughout the entire system could broaden the relaxation time distribution as some segments may have formed one or two hydrogen bonds while others may be in an environment where such intermolecular interactions are minimal [25]. Segments with different degrees of coupling will exhibit different relaxation times, thus broadening the $G(\tau)$ curves of degraded samples.

All the above observations support the interpretation of the weight loss measurement results that were reported earlier, which showed non-significant degradation up to 75 d after which considerable degradation had taken place at 145 d [5].

4. Conclusions

The relaxation signature on dielectric loss permittivity vs. frequency curves of hydrolytically degraded carboxylic acid-terminated poly(D,L-lactide) samples is considerably more distinct than those of undegraded samples. Specifically, for both degraded and undegraded samples, there is a glass transition relaxation peak at temperatures just beneath a DSC-based glass transition midpoint, assigned to the α process, which becomes more distinct and shifts to higher frequency with increased temperature. In addition, there is a linear section in the low frequency regime on log–log ε'' vs. f plots that is attributed to d.c. conductivity which shifts upward with increasing degradation time and is most likely related to the increased concentration of COOH groups resulting from ester linkage hydrolysis with increased chain scission. The upward shift in f_{max} was not great up to 75 d but is considerable after 145 d of degradation, which implies a decrease in the time scale of long range chain segmental motions with increased degradation time.

Experimental dielectric data for degraded and undegraded materials were fitted to the Havriliak–Negami equation with subtraction of the d.c. conductivity contribution to uncover pure relaxation peaks. Relaxation parameters extracted from these fits were used to construct VFTH and distribution of relaxation time curves for all samples. The relaxation time of the α-transition in both degraded and undegraded samples showed VFTH temperature behavior. Values of the Vogel temperature decreased with immersion in buffer for 75 d but then increased for samples immersed for 145 d. This was rationalized in terms of excess free volume associated with chain ends and the out-leaching of oligomers at longer degradation times.

Distribution of relaxation time curves broadened with degradation and shifted to lower times, which can be explained in terms of a broadening of molecular weight by hydrolytic scission as well as faster chain motions. In the future, GPC or MALDI-TOF experiments will be conducted so as to compare the distribution of relaxation times with the molecular weight distribution. Thus, it is concluded that the technique of modern broadband dielectric spectroscopy can be a powerful tool in assessing the fundamental molecular events underlying material biodegradation. Future studies will involve a greater number of degradation times, degradation temperatures, and aqueous electrolyte compositions.

Acknowledgements

The authors gratefully acknowledge The Office of Naval Research Grant No. N00014-04-1-0703 for financial support, and ORTEC Inc., Easley, S.C., for supplying D,L-lactide monomer used in the synthesis of the polymer.

References

[1] Yu F, Zhuo R. Polym J 2003;35:671–6.
[2] Lee S, Kim S, Han Y, Kim Y. J Polym Sci Part A Polym Chem 2001;39:973–85.
[3] Tracy M, Ward K, Firouzabadian L, Wang Y, Dong N, Qian R, et al. Biomaterials 1999;20:1057–62.
[4] Huffman K, Casey D. J Polym Sci Part A Polym Chem 1985;23:1939–54.
[5] Wiggins JS, Hassan MK, Mauritz KA, Storey RF. Polymer 2006;47:1960.
[6] Schönhals A, Kremer F. In: Kremer F, Schönhals A, editors. Broadband dielectric spectroscopy. Berlin: Springer; 2003. p. 225.
[7] Henry F, Costa LC, Devassine M. Eur Polym J 2005;41:2122–6.
[8] Cole KS, Cole RH. J Chem Phys 1941;9:341.
[9] Havriliak S, Negami S. J Polym Sci Polym Symp 1966;14:99.
[10] Havriliak S, Negami S. Polymer 1967;8:161.
[11] Negami S, Ruch RJ, Myers RR. J Colloid Interface Sci 1982;90:117.

[12] McCrum NG, Read BE, Williams G. Anelastic and dielectric effects in polymeric solids. New York: Dover; 1991.
[13] Mauritz KA, Fu R-M. Macromolecules 1988;21:1324–33.
[14] Mauritz KA. Macromolecules 1989;22:4483–8.
[15] Deng ZD, Mauritz KA. Macromolecules 1992;25:2369–80.
[16] Mauritz KA, Yun H. Macromolecules 1989;22:220–5.
[17] Mauritz KA, Yun H. Macromolecules 1988;21:2738–43.
[18] Deng ZD, Mauritz KA. Macromolecules 1992;25:2739–45.
[19] Jamshidi K, Hyon S-H, Ikada Y. Polymer 1988;29:2229.
[20] Fox TG, Flory PJ. J Appl Phys 1950;21:581.
[21] Fox TG, Flory PJ. J Polym Sci 1954;14:315.
[22] Zhang S, Painter PC, Runt JP. Macromolecules 2004;37:2636.
[23] Vogel H. Phys Z 1921;22:645; Tammann G, Hesse W. Z Anorg Allg Chem 1926;156:245; Fulcher GS. J Am Ceram Soc 1923;8:339.
[24] Schönhals A. In: Runt JP, Fitzgerald JJ, editors. Dielectric spectroscopy of polymeric materials: Fundamentals and applications. Washington, DC: ACS Publications; 1997. p. 89.
[25] Zhang S, Painter PC, Runt JP. Macromolecules 2002;35:9403.
[26] Zetsche A, Fisher EW. Acta Polym 1994;45:168.
[27] Katana G, Fisher EW, Hack T, Abetz V, Kremer F. Macromolecules 1995;28:2714.
[28] Roland CM, Ngai KL. Macromolecules 1991;24:2261.